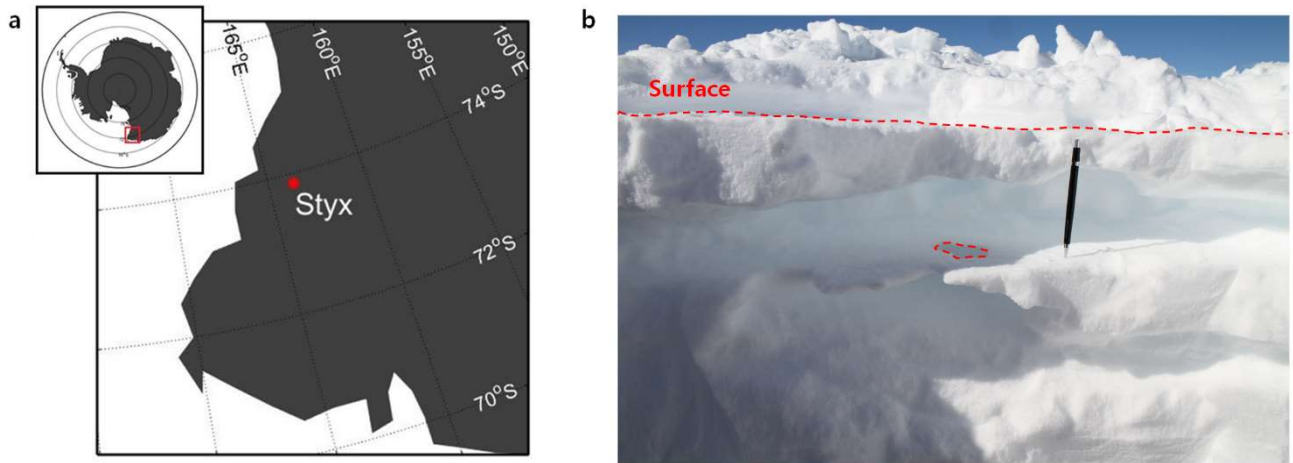


1



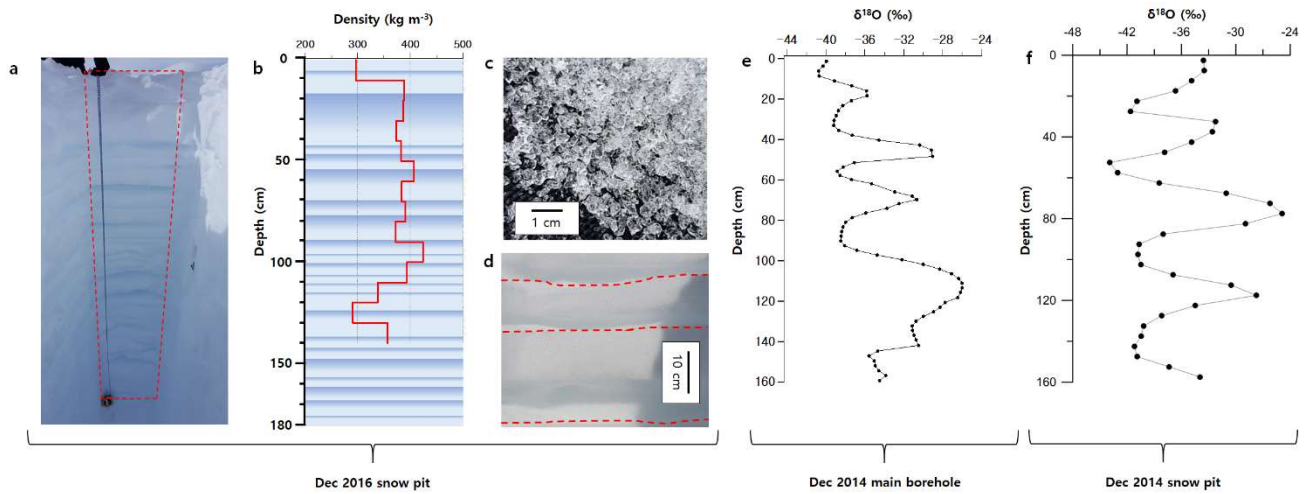
2

3 **Figure 1. (a) Location map of study site, Styx Glacier, Antarctica and (b) a photo of surface snow density**
4 **layers.** The thickness of the snow density layers varies horizontally. The top boundaries of the high-density
5 layers are sharp (horizontal red-dashed line). A hole on a high-density layer surface is indicated by a red-dashed
6 circle. The length of the black sharp pencil in (b) is 14.3 cm.

7

8

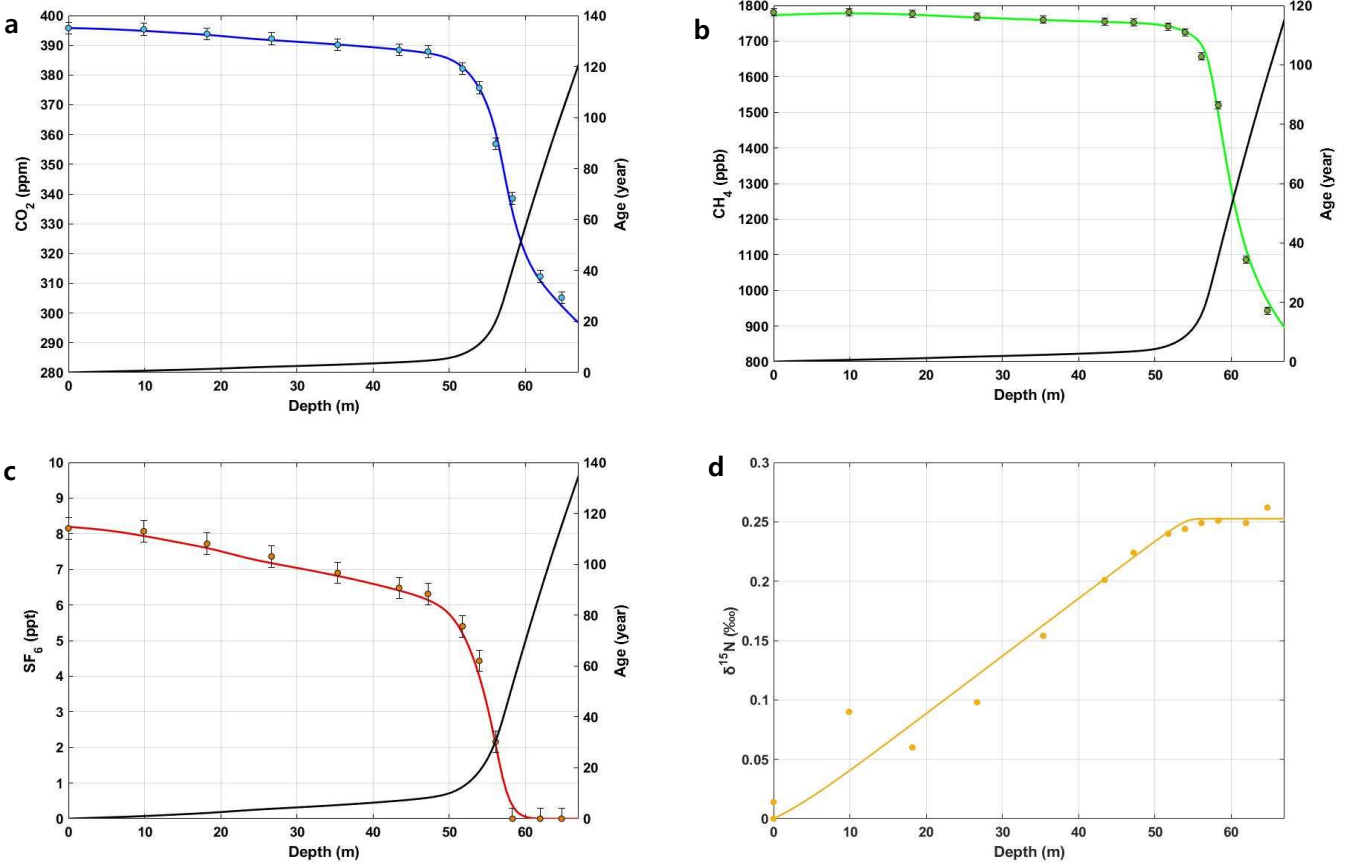
9



11

12 **Figure 2. Snow-pit photos at Styx Glacier. (a) The snow pit with dimensions of $280 \times 65 \times 220$ cm (length**
 13 **\times width \times height). (b) The illustration of qualitatively defined hard (dark blue) and soft (pale blue) layers**
 14 **observed in the top 180-cm-depth interval. Progressive blue color changes indicate a gradual density**
 15 **decrease with depth. Red line is a 10-cm-resolution density profile. (c) Coarse grains observed in a soft**
 16 **layer. (d) Enlarged snow layers. Dashed red lines indicate top boundaries of fine-grained hard layers. (e)**
 17 **and (f) Stable isotope ratio ($\delta^{18}\text{O}$) of snow profiles at the main core and a snow pit 100 m away from the**
 18 **main ice core borehole, respectively.**

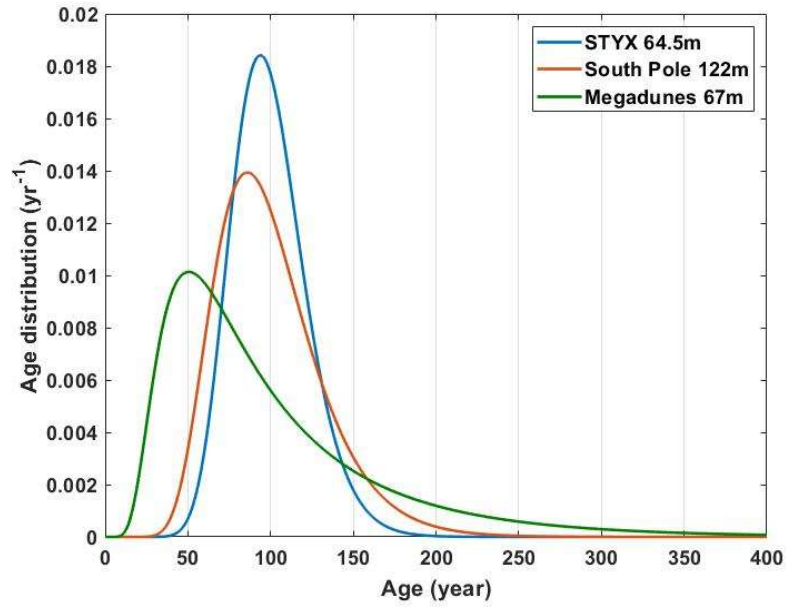
19



21

22 **Figure 3. CO₂, CH₄, SF₆ mole fractions and δ¹⁵N of N₂ measurements (circles), and model results (solid**
 23 **line) for the Styx firn air (air in open porosity). Black lines are modeled ages for the gas species.**

24



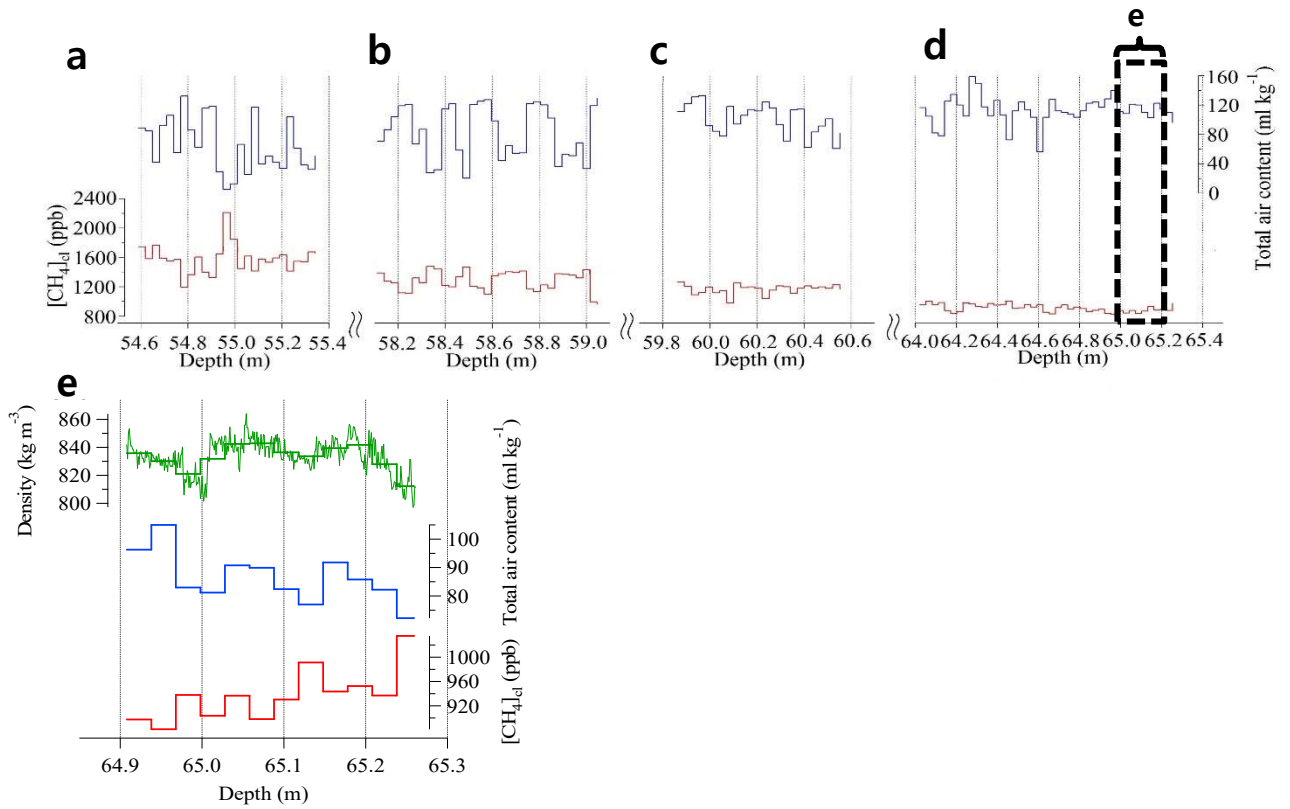
25

26

27 **Figure 4. Comparison of model-simulated CO₂ age distributions at Styx (this study), South Pole (Battle**
28 **et al., 1996), and Megadunes (Severinghaus et al., 2010).**

29

30

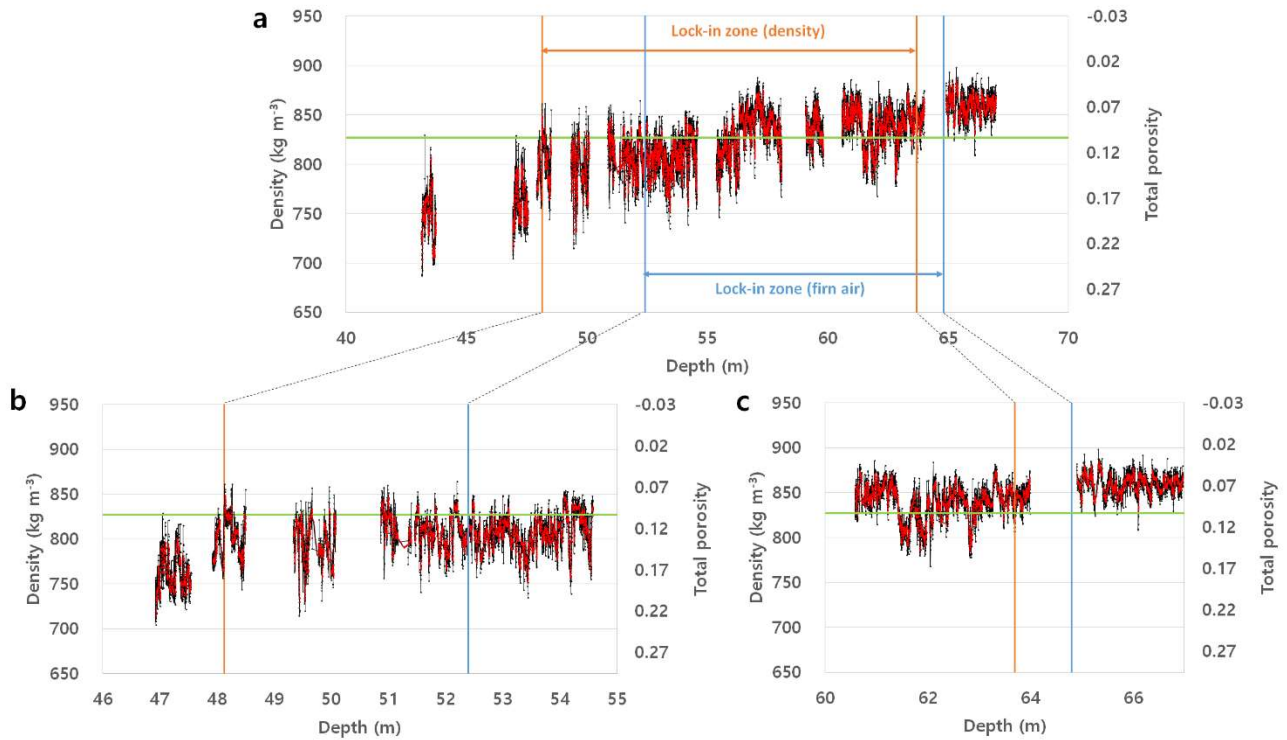


32

33

34 **Figure 5. (a-d) CH₄ mole fraction in closed pores ([CH₄]_{cl}) (red line) and total air content (air volume per**
 35 **ice weight) (blue line) in the lock-in zone of Styx Glacier. (e) Comparison of density with [CH₄]_{cl} and total**
 36 **air content near z_{COD}. A small dashed-box in (d) indicates the depth interval of Fig. 5e.**

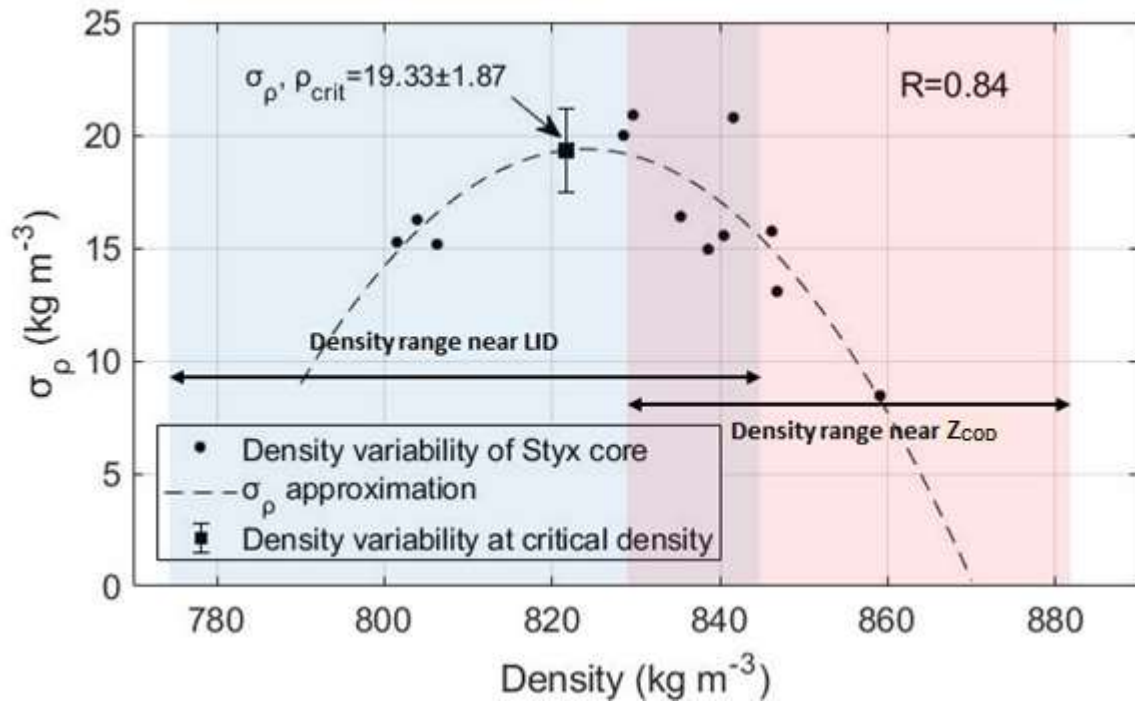
37



39

40 **Figure 6. X-ray high-resolution density data obtained from the lock-in zone. (b) and (c) are enlarged**
 41 **portion of (a). Black lines show individual density data, while the red lines are 1-cm running means. Blue**
 42 **and orange lines represent the boundaries of the LIZ estimated from the gas compositions (between two**
 43 **vertical blue lines) and the critical porosity thresholds (between two orange vertical lines), respectively**
 44 **(see section 3.4).**

45



47

48

49 **Figure 7. Density variability calculated from 1000 depth points and their average density. The standard**

50 **deviation at the critical density (821.68 kg m^{-3}) calculated from the approximate second order polynomial**

51 **($R = 0.84$) is $19.33 \pm 1.87 \text{ kg m}^{-3}$. The blue and red areas are the density ranges near the LID (52.38 -**

52 **52.48 m) and the Z_{COD} (64.91 - 65.01 m), respectively.**

53

Table 1. Glaciological characteristics of Styx Glacier and other firn air sampling sites.

Site	T (°C)	A (cm ice yr ⁻¹)	Effective CO ₂ age (year)	LID (m)	COD (m)	LIZ thickness (m)	References
Styx	-31.7	10	93	52.4	64.8	12.4	This study, Yang et al. (2018)
Megadunes	-49	~0	129	64.5	68.5	4	Severinghaus et al. (2010)
South Pole	-51.0	8	91	115	125	10	Severinghaus et al. (2001)
Siple Dome	-25.4	13	59	49	58	9	Severinghaus et al. (2001)
Dome C	-54.5	2.7	33	97	100	3	Landais et al. (2006)
WAIS Divide	-31	22	39	~67	76.5	9.5	Battle et al. (2011)
NEEM	-28.9	22	50	63	78	15	Buizert et al. (2012a)
NGRIP	-31.1	19	45	67.5	78	11.5	Kawamura et al. (2006)
Summit	-32	23	26	70	80.8	10.8	Witrant et al. (2012)
DE-08	-19	120	13	71.8	88.5	16.8	Etheridge et al. (1996)

57 **Table 2. Comparison of standard deviation of density (σ_ρ) at critical density (ρ_{crit}). For data from all other**
58 **sites, except the Styx, refer to Hörhold et al. (2011).**

59

Campaign/Region	Core name	ρ_{crit} (kg m ⁻³)	$\sigma_\rho, \rho_{\text{crit}}$ (kg m ⁻³)	T (°C)	A (cm ice yr ⁻¹)
Styx	Styx	821.68	19.33±1.87	-31.7	10
NGT	B16	819.27	12.26	-27	15.5
NGT	B18	820.81	12.81	-30	11.3
NGT	B21	820.81	12.91	-30	11.8
NGT	B26	820.85	13.23	-30.6	20
NGT	B29	821.32	10.50	-31.6	16.7
Berkner Island	B25	819.16	14.57	-27	15
DML	B31	827.00	10.27	-42	6.9
DML	B32	827.00	11.28	-42	6.7
DML	B36/37	827.50	8.12	-44.6	7.3
Pre-IPICS	B38	815.00	16.59	-18.1	136
Pre-IPICS	B39	814.91	17.11	-17.9	84
Pre-IPICS	DML95	815.51	13.42	-19.2	60
Pre-IPICS	DML97	816.07	10.03	-20.4	53
Dome C	EDC2	832.02	4.59	-53	2.7
WAIS Divide	WDC06A	820.81	10.35	-31	22

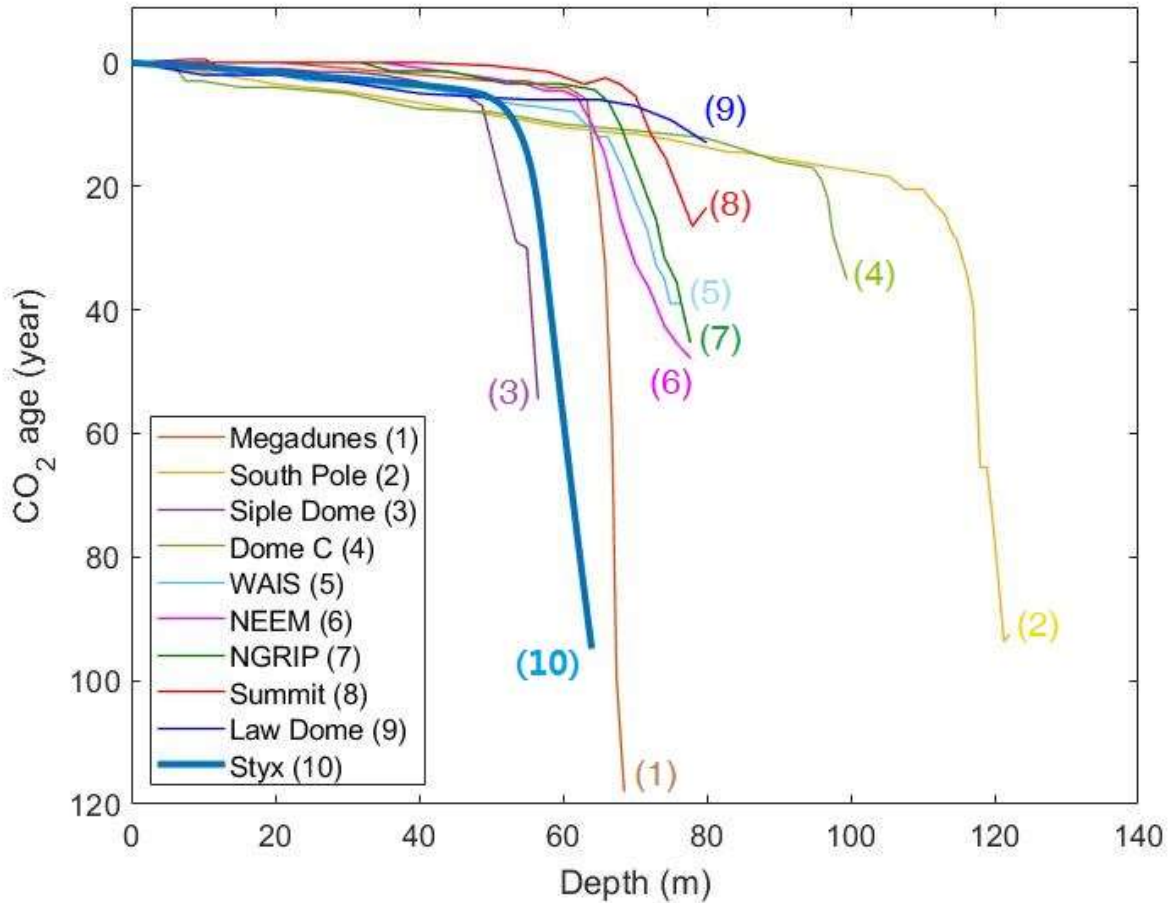
60

61

62 Supplement Materials

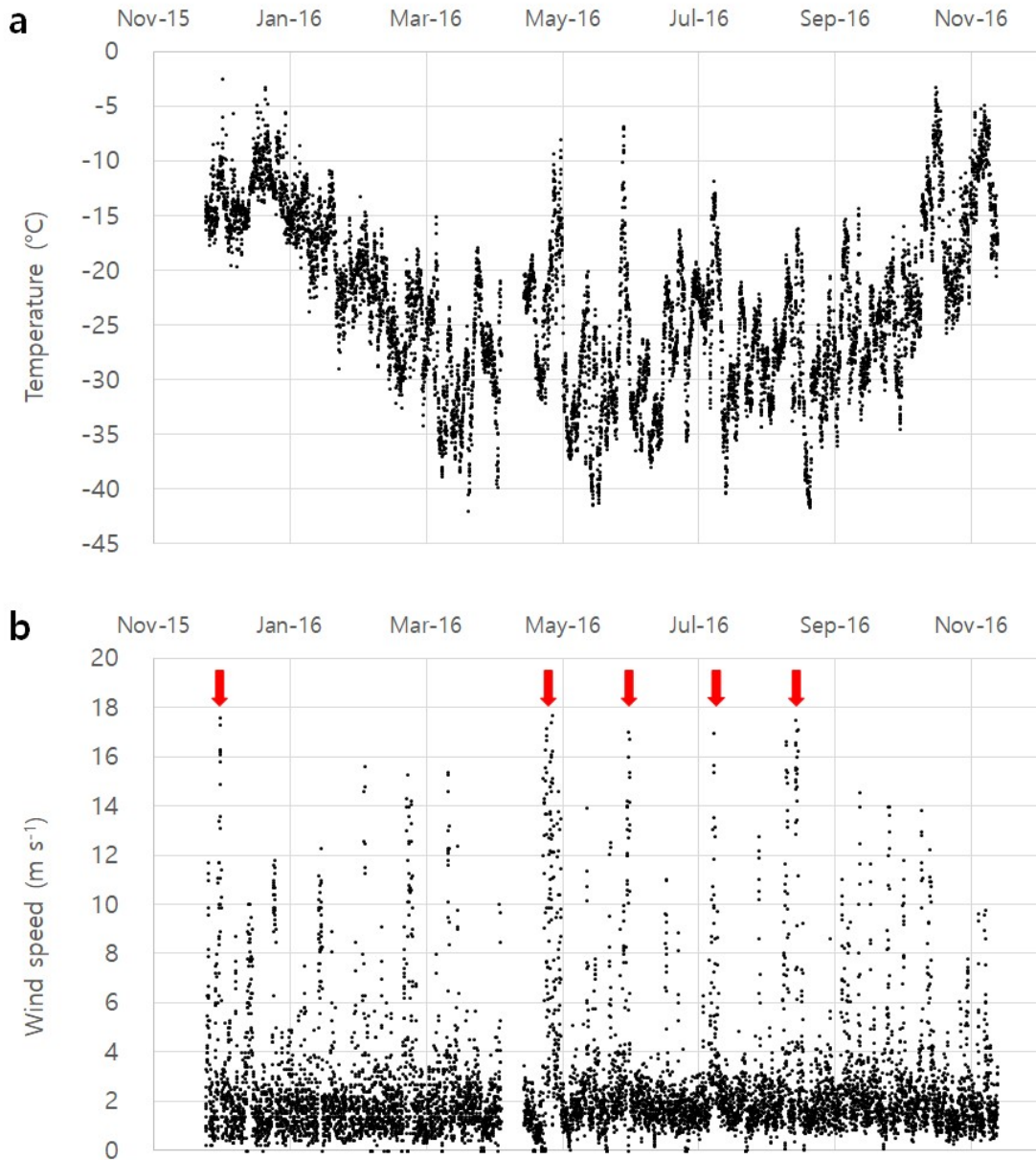
63

64



65

66 **Figure S1. Comparison of CO₂ ages at several firn air sampling sites in Antarctica and Greenland. Old**
67 **firn air (>55 years) is reported only in inland sites, where temperatures and snow accumulation rates**
68 **are relatively low. However, 93-year old firn air was observed at Styx Glacier, where the coast is near**
69 **and snow accumulation rates are high. References: (1) Severinghaus et al. (2010); (2) Battle et al. (1996);**
70 **(3) Severinghaus and Battle. (2006); (4) Landis et al. (2006); (5) Battle et al. (2011); (6) Buizert et al.**
71 **(2012a); (7) Kawamura et al. (2006); (8) Witrant et al. (2012); (9) Etheridge et al. (1996); (10) this study.**



72

73 **Figure S2. (a) Surface air temperature and (b) wind speed data from AWS (Automatic Weather System)**

74 **at Styx Glacier during December 2015 to December 2016. Red arrows indicate blizzard events.**

75